Void Closure by Viscous Flow During Coalescence of Hard Latex Particles

ÖNDER PEKCAN, MURAT CANPOLAT

Department of Physics, Istanbul Technical University, Maslak 80626, Istanbul, Turkey

Received 14 May 1996; accepted 30 July 1996

ABSTRACT: Steady state fluorescence (SSF) technique was used to study the void closure process during coalescence of hard latex particles. Latex films were prepared by annealing pyrene (P_y)-labelled poly(methyl methacrylate) particles above the glass transition temperature. During the annealing processes, the optical clarity of the film increased considerably. Direct fluorescence emission from excited pyrene was monitored as a function of annealing temperature to detect these changes. Scanning electron microscopy in conjunction with Monte Carlo simulations of photon diffusion in latex film were used to interpret the fluorescence results. Void Closure temperature (T_c) and time (t_c) were measured at the point at which the fluorescence emission intensity becomes maximum. This was associated with the longest optical path of a photon in latex film. © 1997 John Wiley & Sons, Inc. J Appl Polym Sci **63:** 651–659, 1997

INTRODUCTION

Coalescence of polymer particles is generally described by the formation of a uniform, homogeneous film by the merger of particles. Coalescence of organic polymers is always performed above the glass transition temperature (T_g) and driven by many different kinds of forces, either intrinsic, such as surface tension, or externally applied as, for example, in compression molding. Particle coalescence in general requires a combination of physical process, such as deformation, interdiffusion, and stress relaxation, which can be distinguished in two different categories. First, a void closure process where molecularly contacting interfaces between particles can be established.[1] Second, interdiffusion of chains across the interface to establish a uniform distribution of entanglements, which is also called equilibration of material.[2] Void closure process is in fact a relaxation of mechanical stresses resulting from deformations of particles.

Latex films are generally formed by coalescence of submicron polymer particles in the form of a colloidal dispersion, usually in water. The term "latex film" normally refers to a film formed from soft latex particles (T_g below room temperature) where the forces accompanying the evaporation of water are sufficient to compress and deform the particles into transparent, void-free film. However, latex films can also be obtained by compression molding of a film of dried latex powder composed of relatively hard polymers, such as polystyrene (PS) or poly (methyl methacrylate) (PMMA), that have T_g above room temperature. Aqueous dispersion of soft latex particles are called low-T, while nonaqueous dispersions of hard polymer particles are generally referred to as high-T. High-T latex particles remain essentially discrete and undeformed during drying. The mechanical properties of such films can be evolved after all the solvent has evaporated by an annealing process which first leads to void closure and then interdiffusion of chains across particle-particle boundaries.

Correspondence to: Ö. Pekcan

Over the last several years, it has become possible to observe latex film formation at the molecular level. Small angle neutron scattering (SANS) has been used to examine deuterated particles in a protonated matrix.[3] More extensive studies have been performed using SANS by Sperling and coworkers[4,5] on compression molded polystyrene latex films. These works covered mostly interdiffusion process during film formation. Alternatively, the process of interparticle polymer interdiffusion has been studied by direct nonradiative energy transfer (DET) using fluorescence decay measurements in conjunction with particles labeled with appropriate donor and acceptor chromophors.[6,7,8,9] This transient fluorescence technique has been used to examine latex film formation of 1 μm diameter high-T (PMMA) particles[6] and of 100 nm diameter low-T poly (buthyl methacrylate) (PBMA) particles.[7,8] These studies all indicate that in the particular systems examined, annealing the films above T_g leads to polymer interdiffusion at the particle-particle junction as the particle interface heals. Stephen Mazur[10] has written a extensive review on coalescence of polymer particles in which he mainly discussed the neck growth mechanisms and its several geometrical approximations before interdiffusion of polymer chains takes place. Recently, DET and the steady state fluorescence (SSF) technique have been used in this laboratory to study interdiffusion processes at the particle-particle junction during film formation by PMMA latex particles.[11–15] In SSF studies, film thickness is more critical than in fluorescence decay measurements. Special attention must be paid to understand the effect of optical clarity during the SSF measurements.

In this paper, void closure process due to viscous flow was studied in films formed from high-T latex particles by monitoring the direct fluorescence emission (I_{op}) intensities from a dye using SSF technique. Latex films were annealed during equal time intervals at elevated temperatures above T_g. Monte Carlo simulations were carried out to calculate the number of scattered (N_{sc}) and emitted (N_{op}) photons from a film by employing photon diffusion theory.[16] The evolution in optical clarity is modeled by the variation in mean free path ($\langle l \rangle$) of a photon in latex films at each annealing step. Scanning electron microscopy (SEM) was used to detect the disappearance of interparticle voids, which then was related to the variation in optical clarity and path (s) of a photon in the latex film. The Vogel–Fulcher equation[17,18] was employed to quantify the temperature dependence of I_{op} during latex formation.

High-T latex particles, with diameters ranging from 1 to 3 μm were used. Each particle consisted of 96 mol % PMMA and 4 mol % polyisobutylene (PIB), which formed an interpenetrating network throughout the particle. The PIB is very soluble in certain hydrocarbon media. A thin layer of PIB serves for stabilization. A pyrene (P) dye was used to label the particles.

THEORETICAL CONSIDERATIONS

Photon Diffusion

The journey of an excited or emitted photon to or from a dye molecule in a film formed from annealed latex particles can be modeled by photon diffusion theory.[16] The collision probability p of a travelling photon with any scattering center in a film is given by

$$P = 1 - \exp(-l/\langle l \rangle) \qquad (1)$$

where l is the distance of a photon between each consecutive collision and $\langle l \rangle$ is defined as the mean free path of a photon. Here, the film is taken as a plane sheet with thickness d, and the direction of incident photons is taken perpendicular to the film surface (in z, the direction).

In Monte Carlo simulations, random collisions can be determined by choosing p randomly in between 0 and 1 ($0 < p < 1$). Then after each collisional step, l is calculated using eq. 1 for a given $\langle l \rangle$ value. The z component of the total distance that a photon travels in the film is then determined by adding the z components of l values that are found from each of the collisional steps by using the relation $S_z = \sum_i^n l_{iz}$, where i labels the successive collisions during the journey of a photon. Photons emerging from the back and front surface of the film without interacting with a pyrene molecule can be determined by using the following conditions

$$s_z > d \quad \text{and} \quad s_z < 0 \qquad (2)$$

respectively, where the front surface of the film is taken at the $Z = 0$ position. The total number of photons emerging from the front surface is then represented by N_{sc}, which is assumed to be pro-

portional to the intensity I_{sc} of the light scattered from latex film during SSF measurements.

In order to derive the relation for the fluorescence intensity, I_{op} emitted from the latex film, we defined the probability of a photon encountering a pyrene molecule as

$$q = 1 - \exp(-s/h) \tag{3}$$

Here, s represents the total distance that the photon travels in the film (optical path), and h is the mean distance the photon travels in the film before it finds a pyrene molecule. If s is large, the probability of the photon encountering a pyrene is high and vice versa. After collision with a pyrene, the photon travels again (eq. 1). Then d is compared with the z component of the total distance s_z (eq. 2) to find if the photon is emitted from the film surfaces. The number of photons emitted from the front surface of the film is given by N_{op}, which is assumed to be proportional to I_{op}, the fluorescence intensity.

In Monte Carlo simulations, h and d were taken to be fixed parameters with the values of 10 and 140, respectively. Here we have to note that h is considered to be inversely proportional to the pyrene concentration in latex film (which is assumed to be constant during the film formation processes). The mean free path $\langle l \rangle$ was varied between 1 to 20 for a given d; and for each $\langle l \rangle$, the number of incident photons was taken to be 3×10^4 during the simulations. The number of collisions n is varied so that the conditions in eq. 2 are satisfied.

Void Closure Kinetics

Dillon et al.[19] were the first to postulate that dry sintering of two particles that are contact with each other occurs through viscous flow of polymer. Then particle deformation and void closure between particles can be induced by shearing stress, which is generated by surface tension of polymer, i.e., polymer air interfacial tension. The void closure kinetics can determine the time for optical clarity and film formation.[20] An expression to relate the shrinkage of spherical void of radius r to the viscosity of surrounding medium η was derived and given by the following relation:[21]

$$\frac{dr}{dt} = -\frac{\gamma}{2\eta}\left(\frac{1}{\rho(r)}\right) \tag{4}$$

where γ is the surface energy, t is time, and $\rho(r)$ is the relative density. It has to be noted that, here, surface energy causes a decrease in void size, and the term $\rho(r)$ varies with the microstructural characteristics of the material, such as the number of voids, the initial particle size, and packing. Here, $\rho(r)$ can be defined as a volume ratio of polymeric material to voids where, as r goes to zero, $\rho(r)$ increases; however for large r values, $\rho(r)$ decreases. Equation (4) is quite similar to one which was used to explain the time dependence of the minimum film formation temperature during latex film formation.[1,22] If the viscosity is constant in time, integration of eq. (4) gives the relation as

$$t = -\frac{2\eta}{\gamma}\int_{r_0}^{r} \rho(r)\, dr \tag{5}$$

where r_0 is the initial void radius at time $t = 0$.

The temperature dependence of viscosity of most amorphous polymers near their T_g can be described by Vogel–Fulcher (VF) equation as[17,18]

$$\eta = A \exp\left(\frac{B}{T - T_0}\right) \tag{6}$$

where A, B, and T_0 are the constants for a given polymer. For most glasses, T_0 is typically about 50°K, lower than T_g. Combining eqs. (5) and (6), the following useful equation is obtained

$$t = -\frac{2A}{\gamma}\exp\left(\frac{B}{T - T_0}\right)\int_{r_0}^{r} \rho(r)\, dr \tag{7}$$

Equation (7) will be employed to interpret the fluorescence data to explain the void closure mechanism in following the sections.

EXPERIMENTAL

P-labeled PMMA-PIB polymer particles were prepared separately in a two-step process. First, MMA was polymerized to low conversion in cyclohexane in the presence of PIB containing 2% isoprene units to promote grafting. The graft copolymer so produced served as a dispersant in the second stage of polymerization, in which MMA was polymerized in a cyclohexane solution of the polymer. Details have been published elsewhere.[23] A stable dispersion of spherical polymer

particles was produced, ranging in radius from 1 to 3 μm. A combination of ^{1}H-NMR (nuclear magnetic resonance) and ultraviolet (UV) analysis indicated that these particles contain 6 mol % PIB and 0.037 mmol *P* groups per gram of polymer. (These particles were prepared by B. Williamson in Prof. M. A. Winnik's Laboratory in Toronto.)

Latex film preparation was carried out in the following manner. The *P*-labeled particles were dispersed in heptane in a test tube. After complete mixing, a large drop of the dispersion was dropped on a round silica window plate with a diameter of 2 cm. The heptane was allowed to evaporate. Then the films were annealed above the glass transition temperature of PMMA for 30 min at temperatures ranging from 110 to 220°C. During annealing, temperature was maintained within ±2°C.

Afterwards, fluorescence experiments were performed. The silica plate was placed in the solid surface accessory of a Perkin Elmer Model LS-50 fluorescence spectrometer. All measurements were carried out in the front face position at room temperature. Slit widths were kept at 2.5 mm. Film thicknesses were measured by weighing the silica plate before and after the film was cast. *P* was excited at 345 nm, and fluorescence emission spectra were detected at room temperature in the 340–500 nm range. Film samples were illuminated only during the actual fluorescence measurements and at all other times were shielded from the light source. In all experiments, maximum peak heights at 345 and 375 nm were used for the scattered and *P* intensities (I_{sc} and I_{op}), respectively. Peak ratios were always checked in the *P* spectra during the experiments.

In fluorescence measurements, errors originate mostly from the surface inhomogeneities (voids and cracks) of film samples, which cause variation in I_{sc} and I_{op} intensities. Signal-to-noise ratio in fluorescence intensities are quite low (1–2%) and can be neglected in error estimations. Here, five to six samples were run under each set of conditions to test the reproducibility of results. Below the healing point, errors in fluorescence intensities were estimated to be about ±10%. Above the healing point, errors decrease to ±5% due to disappearance of surface inhomogeneities. Errors in times simply come from the chronometer, and this increases at shorter time intervals.

Scanning electron micrographs were taken at 10–15 kV in JEOL JSM microscope. A Hummer VII sputtering system was used for gold coating of latex films.

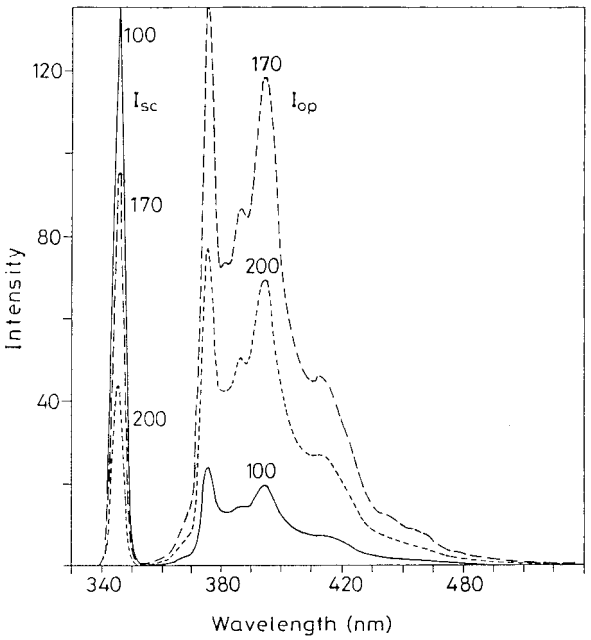

Figure 1 Emission (I_{op}) and scattered (I_{sc}) spectra of pyrene, after latex film sample was annealed at 100 (——), 170 (----), and 200°C (· · · · ·) for 30 min intervals and excited at 345 nm.

RESULTS AND DISCUSSION

Optical Clarity and Void Closure

Typical emission (I_{op}) and scattered (I_{sc}) spectra of a latex film are shown in Figure 1. Upon annealing, *P* intensity (I_{op}) first increased and reached a maximum at 150°C, then decreased. However, I_{sc} decreased continuously above 120°C with increasing annealing temperature. I_{op} and I_{sc} versus annealing temperature are plotted in Figure 2(a) and (b).

The variation in I_{op} depends on the mean optical path *s* of a photon in the film. This mean optical path is directly proportional to the probability of the photon encountering a pyrene molecule. Before annealing, the photon is scattered from the particle surfaces. That is, the mean free path ($\langle l \rangle$) is of the order of the size of the particle and interparticle voids. After a few steps, the photon reemerges from the front surface of the film. Thus, the mean optical path *s* is very short. After the void closure process is completed, scattering takes place predominantly from the interparticle interfaces, and the mean free path is of the order of the deformed particle size. In this regime, (with the same number of rescatterings), a photon will stay for a much longer time in the film, and I_{op} will

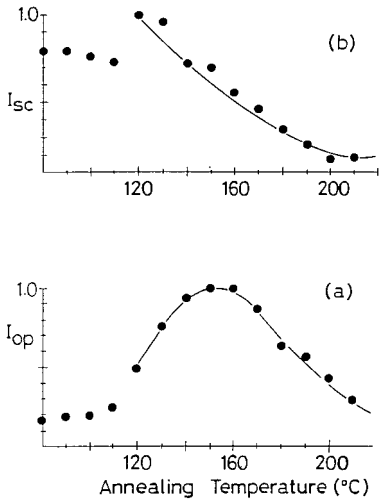

Figure 2 Normalized $a - I_{op}$ and $b - I_{sc}$ intensities versus annealing temperature for latex film samples.

increase. After the completion of the void closure process, these interfaces are removed by interdiffusion of chains.[10,11] The film becomes essentially transparent to the photon, the mean free path diverges, and s is of the order of the film thickness d.

The maximum in I_{op} can be explained by the void closure process at the interparticle interface. The time (30 min) can be referred to as the void closure time (t_c) at 150°C, during which polymeric material occupies the interparticle voids. At this temperature (T_c) and time, t_c interparticle voids disappear, and the latex film starts to become semitransparent to the exciting light for P molecules. As a result, the emission intensity I_{op} reaches a maximum. At 210°C, complete transparency is reached due to complete annealing of latex film with the disappearance of all interparticle interfaces. It is here that the I_{op} decreases once more.[10,11]

We have demonstrated, by means of Monte Carlo simulations to be discussed below, that merely the film thickness represents a much shorter value then the optical path, that obtained by multiple scattering from interparticle interfaces after the void closure process is completed.

Simulation of Photon Diffusion in Latex Film

These speculations can be modeled and the behavior of I_{op} and I_{sc} can be interpreted by results of Monte Carlo simulations. N_{op} and N_{sc} are plotted versus mean free path $\langle l \rangle$ of a photon in Figure 3(a) and (b). Here, N_{op} first increases then decreases by increasing $\langle l \rangle$, which indicates that for intermediate $\langle l \rangle$ values, the optical path s of a photon is longest and the probability of encountering a pyrene in the film is highest. As a result, N_{op} reaches a maximum. However, for shorter and longer $\langle l \rangle$ values, the photons can easily escape from the front and back surfaces of the film, respectively. As a result, the number of back scattered photons N_{sc} decreases continuously with increasing $\langle l \rangle$ values.

In order to support these findings, scanning electron micrographs (SEM) of latex films were taken before and after annealing above T_g for 30 min. Figure 4(a) shows the SEM result of a powder film before annealing; Figure 4(b) presents a micrograph of a film annealed at 140°C, at which voids have disappeared, but with some structure related to particle interfaces. A transparent film obtained by annealing at 180°C is shown in Figure 4(c).

SEM results are found to be consistent with the photon diffusion model. Schematic figures of film formation by high-T latex particles and its relationships with the mean free and optical paths ($\langle l \rangle$ and s) are presented in Figure 5. The early stage of film formation is shown in Figure 5(a), where close packed particles form a powder film that includes many voids. This film yields low I_{op} and high I_{sc} values due to short $\langle l \rangle$ and s lengths. Figure 5(b) presents a film on which, due to annealing, interparticle voids start to disap-

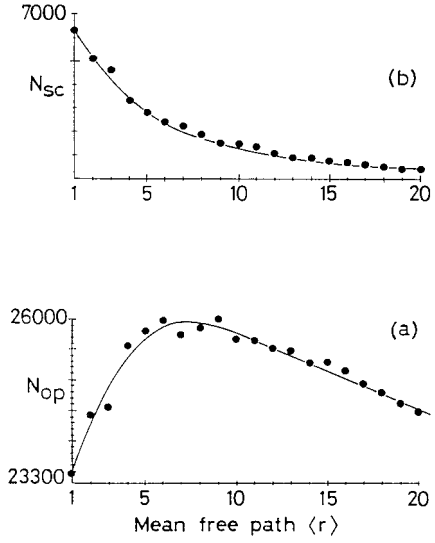

Figure 3 Plot of Monte Carlo simulations: (a) N_{op} and (b) N_{sc} versus mean free path $\langle l \rangle$ of a photon in film of thickness $d = 100$.

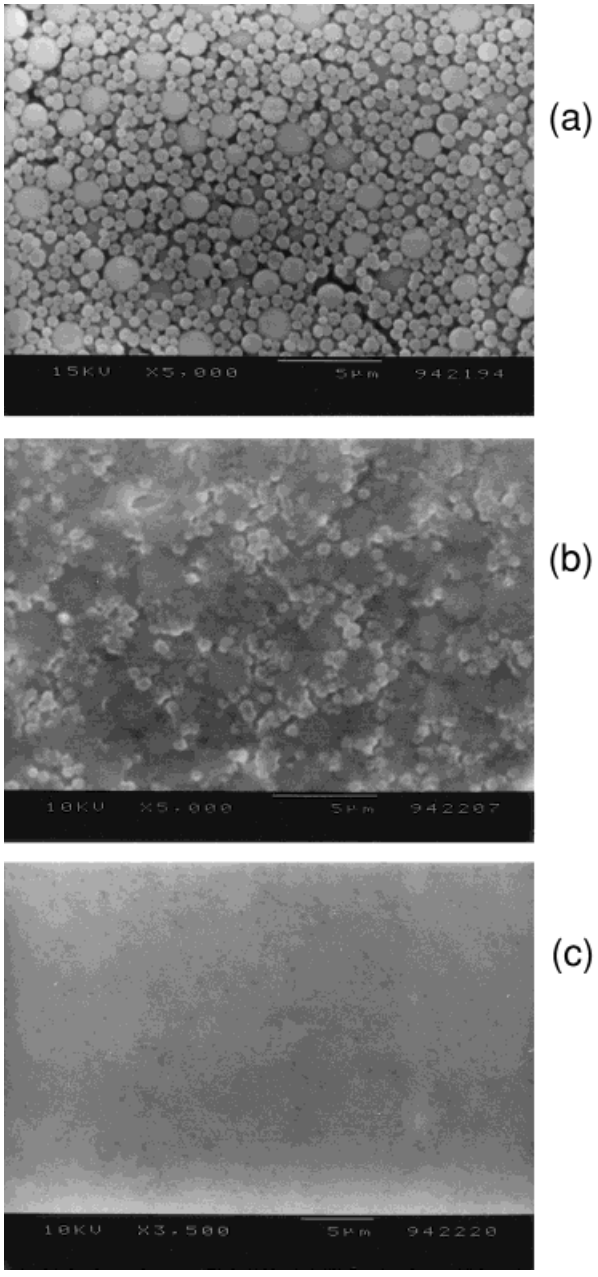

Figure 4 Scanning electron micrographs of latex films, annealed for 30 min at (a) 25, (b) 140, and (c) 180°C.

pear, which gives rise to higher $\langle l \rangle$ and the longest s values. In such a film, one can observe high I_{op} and low I_{sc} intensities. Finally, Figure 5(c) shows a fully transparent film with the longest $\langle l \rangle$ but smaller s values. This film has low I_{op} and I_{sc} intensities.

Void Closure During Latex Film Formation

Based upon SSF and SEM results in conjunction with Monte Carlo simulations, it appears that the evolution of the optical clarity during film formation from high-T latex particles is related to the void closure process. It is possible to obtain a quantitative value from these observations. A similar behavior for I_{op} was observed for other latex film samples that were annealed at other time intervals. However, the maximum in I_{op} is shifted to higher temperatures for shorter annealing times. When the film was annealed for 90 min, the maximum in I_{op} appeared at 130°C. However, as the annealing time decreased (40, 30, 15, 10, and 5 minutes), the temperature for the maximum in I_{op} increased (140, 150, 160, 180, and 210°C, respectively). Figure 6(a)–(c) presents the results for samples annealed at elevated temperatures for 15, 10, and 5 min.

In the previous section, the maximum in I_{op} was already explained in terms of the void closure process, where polymeric material flows and fills up the interparticle voids. The maximum in each experimental set corresponds to the void closure time (t_c) for a given temperature or the void closure temperature (T_c) for the time required for the polymeric material to flow into the voids. For instance, at 160, 180, and 210°C, t_c values were

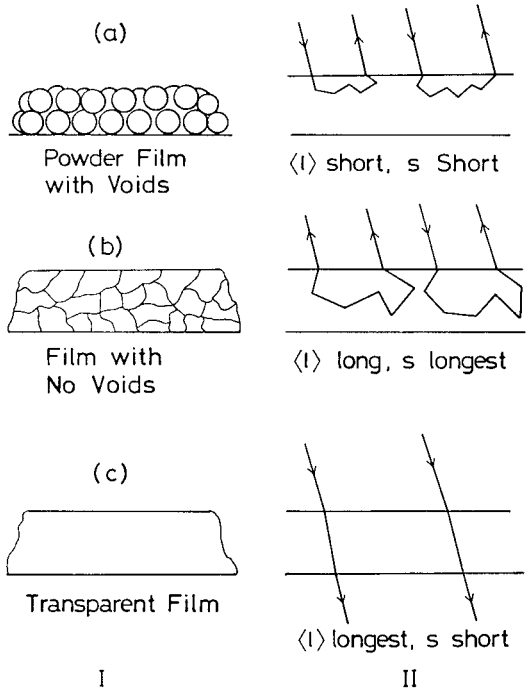

Figure 5 Schematic illustration of the (I) film formation from high-T latex particles and (II) variation in mean free and optical paths ($\langle l \rangle$ and s) during film formation; (a), (b), and (c) correspond to the film formation stages explained in the text.

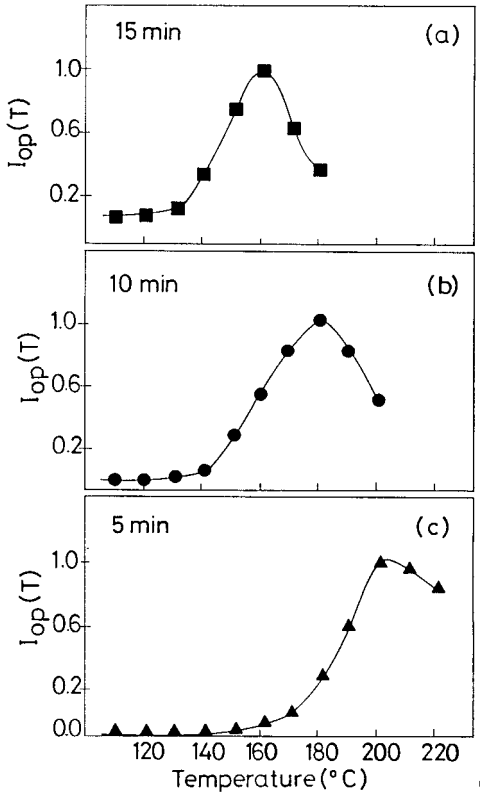

Figure 6 Plot of I_{op} versus annealing temperature for films annealed in (a) 15, (b) 10, and (c) 5 min intervals.

found to be 15, 10, and 5 min, respectively. At 130°C, the maxima in I_{op} for the corresponding time intervals does not differ. This may indicate that, at this temperature, the void closure times do not change when the time intervals are increased.[14,15] In other words, 130°C is the minimum required temperature for the void closure in high-T latex particles during film formation. For a given t_c and T_c, interparticle voids completely disappear due to viscous flow. As a result, I_{op} reaches a maximum.

In order to quantify the above results, eq. (7) can be employed by assuming that the interparticle voids are in equal size and the number of voids stays constant during film formation (i.e., $\rho(r) \propto r^{-3}$), integration of eq. (7) gives the relation

$$t = \frac{2AC}{\gamma} \exp\left(\frac{B}{T - T_0}\right)\left(\frac{1}{r^2} - \frac{1}{r_0^2}\right) \qquad (8)$$

where C is a constant related to relative density $\rho(r)$. As we stated before, a decrease in void size (r) causes an increase in mean free path $\langle l \rangle$ of a photon, which then results an increase in I_{op} intensity. This picture can also be visualized by Frenkel's neck formation model,[24] which takes into account the identical contacting spheres under the influence of surface tension. Frenkel's model assumes that the displaced volume is redistributed uniformally such that the remaining surfaces keep their spherical shapes but of larger radii, which offers a larger mean free path $\langle l \rangle$ of a photon during its journey in the latex film. Figure 7 illustrates Frenkel's picture for neck formation process from latex particles. If the assumption is made that I_{op} is inversely proportional to the void radius r, then eq. (8) can be written as

$$t = \frac{2AC}{\gamma} \exp\left(\frac{B}{T - T_0}\right) I_{op}^2 \qquad (9)$$

Here, r_0^{-2} is omitted from the relation since it is very small compared to r^{-2} values after void closure processes start. Equation (9) can be solved for I_{op} to interpret the results in Figure 6, as

$$I_{op} = S(t) \exp\left(-\frac{B}{2(T - T_0)}\right) \qquad (10)$$

where $S(t) = (\gamma t/2AC)^{1/2}$. For a given time, the logarithmic form of eq. (10) is given as follows:

$$\ln I_{op} = \ln S(t) - \frac{B}{2(T - T_0)} \qquad (11)$$

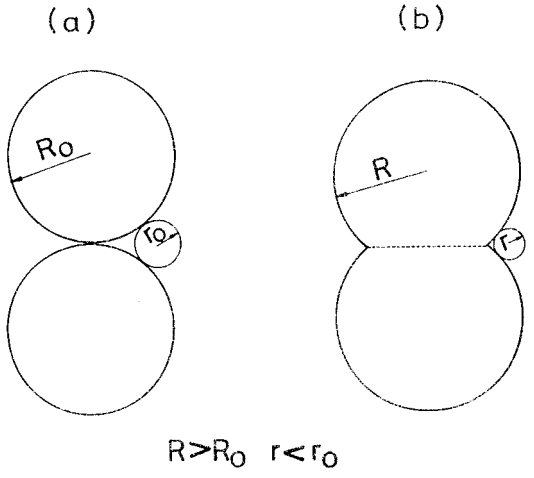

Figure 7 Geometrical illustration of Frenkel's neck growth model between identical particles: (a) before and (b) after neck growth. R_0, R, and r_0 are the particle and void radii before and after neck growth, where $R > R_0$ and $r_0 > r$.

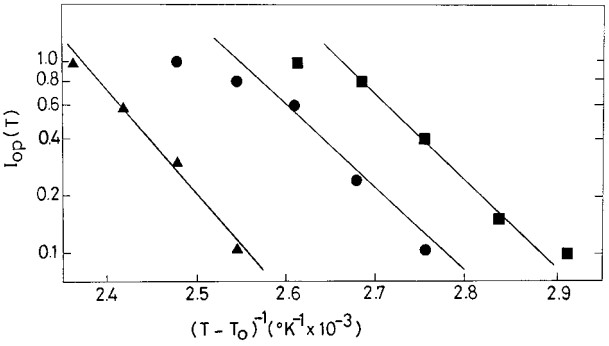

Figure 8 Fit of the data in Figure 6 to eq. (11). Slopes of the curves produce B values.

Data in Figure 6 are fitted to eq. (11), and B values are obtained from the slopes of the straight lines in Figure 8. The averaged B value is found to be 16×10^3°K, which is four times larger than that found for an acrylic[25] (4×10^3°K), and eighty times larger than that found for waterborne acrylic latices.[20,26] The smaller value for a copolymer of MMA and 2-ethyl hexyl acrylate latices was attributed to the plasticizing effect of water.[20] In our case, no such plasticizing effect is expected because our PMMA latex has glass transition of 380°K, which is very high compare to waterborne acrylic latices ($T_g \approx 280$°K). As a result, the value of $B = 16 \times 10^3$°K for our system seems to be quite reasonable for hard latex particles. Here, it has to be noted that curves in Figure 8 are plotted up to the maxima, i.e., void closure temperature T_c. The right-hand side of the curves in Figure 6 present the interdiffusion processes during film formation.

The maximum values of I_{op} in Figure 6 correspond to the (t_c, T_c) pairs, at which eq. (8) can be written as

$$t_c = S(r_c)\exp\left(\frac{B}{T_c - T_0}\right) \qquad (12)$$

where $S(r_c) = 2AC/\gamma r_0^2$. Here, r_c is the critical void radius at which optical path of a photon becomes longest in the latex film. As soon as r_c reaches zero, chain interdiffusion (i.e., equilibration) starts at deformed particle-particle interfaceses.[14,15] (t_c, T_c) data are plotted in Figure 9 and fitted to the logarithmic form of eq. (12). B is produced from the slope of the straight line in Figure 10 and found to be 7×10^3°K, which is two times smaller that found by using eq. (11). At this stage of our work, we are unable to interpret this difference between B values. However, one may argue that B value found from eq. (12) may be the critical one at the final stage of the void closure process where the polymeric material

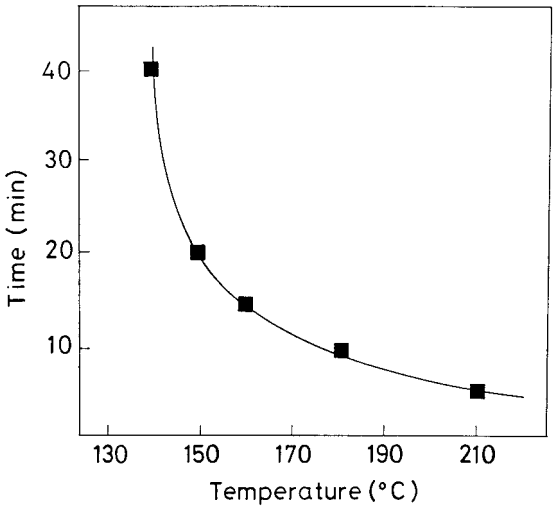

Figure 9 Plot of annealing time versus temperature for the maxima of I_{op} intensities.

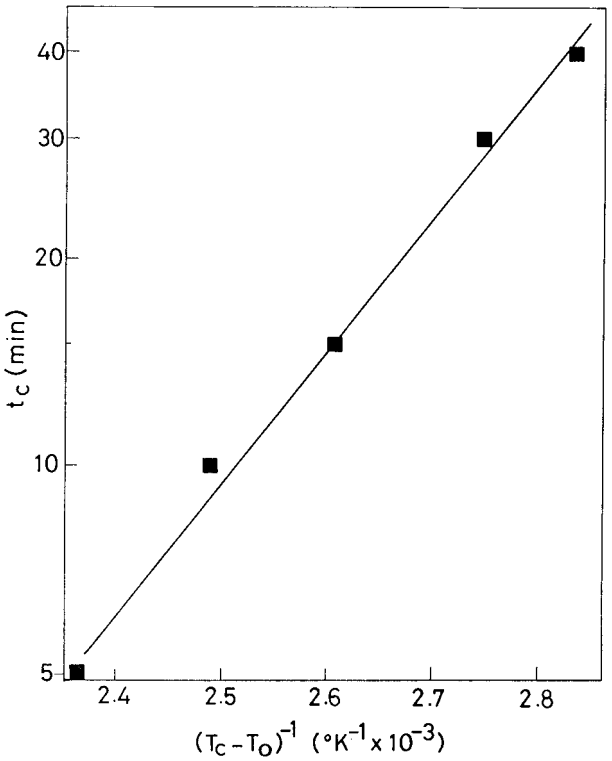

Figure 10 Data in Figure 9 are fitted to eq. (12), where t_c and T_c are named as void closure time and temperature given in text. The slope of the curve produced B value.

needs less effort to flow to fill the critical void with radius r_c.

CONCLUSION

In conclusion, this work employed photon diffusion theory in conjunction with SEM to study void closure process during film formation from high-T latex particles. We have shown that a simple kinetic model for void closure mechanism is fitted well to our fluorescence data; however, much of work has to be done to find more reliable explanation at the critical point (t_c, T_c).

We thank Professor M. A. Winnik for supplying us with the latex material and his stimulating ideas.

REFERENCES

1. P. R. Sperry, B. S. Snyder, M. L. O'Dowd, and P. M. Lesko, *Langmuir,* **10,** 2619 (1994).
2. H. H. Kausch and M. Tirrell, *Ann. Rev. Mater. Sci.,* **19,** 341 (1989).
3. K. Hahn, G. Ley, H. Schuller, and R. Oberthur, *Coll. Polym. Sci.,* **66,** 631 (1988).
4. J. N. Yoo, L. H. Sperling, C. J. Glinka, and A. Klein, *Macromolecules,* **23,** 3962 (1990).
5. K. D. Kim, L. H. Sperling, and A. Klein, *Macromolecules,* **26,** 4624 (1993).
6. Ö. Pekcan, M. A. Winnik, and M. D. Croucher, *Macromolecules,* **23,** 2673 (1990).
7. C. L. Zhao, Y. Wang, Z. Hruska, and M. A. Winnik, *Macromolecules,* **23,** 4082 (1990).
8. Y. Wang, C. L. Zhao, and M. A. Winnik, *J. Chem. Phys.,* **95,** 2143 (1991).
9. E. M. Boczar, B. C. Dionne, Z. Fu, A. B. Kirk, P. M. Lesko, and A. D. Koller, *Macromolecules,* **26,** 5772 (1993).
10. S. Mazur, *Polymer Powder Technology,* M. Maukis and V. Rosenweig, Eds., John Wiley and Sons, 1996.
11. Ö. Pekcan and M. Canpolat, *J. Appl. Polym. Sci.,* **59,** 277 (1996).
12. Ö. Pekcan, M. Canpolat, and A. Gocmen, *Polymer,* **34,** 3319 (1993).
13. M. Canpolat and Ö. Pekcan, *Polymer,* **36,** 4433, (1995).
14. Ö. Pekcan, *Trends in Polymer Science,* **2,** 236 (1994).
15. M. Canpolat and Ö. Pekcan, *Polymer,* **36,** 2025 (1995).
16. G. H. Meeten, *Optical Properties of Polymers,* Elsevier, New York, 1989.
17. H. Vogel, *Phys. Z.,* **22,** 645 (1925).
18. G. S. Fulcher, *J. Am. Ceram. Soc.,* **8,** 339 (1925).
19. R. E. Dillon, L. A. Matheson, and E. B. Bradford, *J. Colloid Sci.,* **6,** 108 (1951).
20. J. L. Keddie, P. Meredith, R. A. L. Jones, and A. M. Ronald, *Proc. Am. Chem. Soc.,* Chicago Mtg., American Chemical Society, Washington, D.C., 1995.
21. J. K. Mackenzie and R. Shuttleworth, *Proc. Phys. Soc.,* **62,** 838 (1949).
22. G. B. McKenna, in *Comprehensive Polymer Science,* Vol. 2, C. Booth and C. Price, Eds., Pergamon Press, Oxford, 1989.
23. M. A. Winnik, M. H. Hua, B. Hongham, B. Williamson, and M. D. Croucher, *Macromolecules,* **17,** 262 (1984).
24. J. Frenkel, *J. Phys. USSR,* **9,** 385 (1945).
25. D. W. Krevelen and P. J. Hoftyzer, *Properties of Polymers, Their Estimation and Correlation with Chemical Structure,* Elsevier, Amsterdam, 1976, p. 343.
26. J. L. Keddie, P. Meredith, R. A. L. Jones, and A. M. Ronald, *Macromolecules,* **28,** 2673 (1995).